Available online at www.sciencedirect.com
ScienceDirect
International Journal of Multiphase Flow 33 (2007) 948–969
International Journal of Multiphase Flow
www.elsevier.com/locate/ijmulflow

Studies on two-phase co-current air/non-Newtonian shear-thinning fluid flows in inclined smooth pipes

Jing-yu Xu [a], Ying-xiang Wu [a,*], Zai-hong Shi [b], Li-yun Lao [c], Dong-hui Li [a]

[a] Division of Engineering Sciences, Institute of Mechanics, Chinese Academy of Sciences, Beijing 100080, China
[b] Petroleum Exploration and Production Research Institute, Sinopec Corp, Beijing 100083, China
[c] BP Institute for Multiphase Flows, University of Cambridge, Madingley Road, Cambridge CB3 0EZ, UK

Received 20 April 2006; received in revised form 28 March 2007

Abstract

In this work, co-current flow characteristics of air/non-Newtonian liquid systems in inclined smooth pipes are studied experimentally and theoretically using transparent tubes of 20, 40 and 60 mm in diameter. Each tube includes two 10 m long pipe branches connected by a U-bend that is capable of being inclined to any angle, from a completely horizontal to a fully vertical position. The flow rate of each phase is varied over a wide range. The studied flow phenomena are bubbly flow, stratified flow, plug flow, slug flow, churn flow and annular flow. These are observed and recorded by a high-speed camera over a wide range of operating conditions. The effects of the liquid phase properties, the inclination angle and the pipe diameter on two-phase flow characteristics are systematically studied. The Heywood–Charles model for horizontal flow was modified to accommodate stratified flow in inclined pipes, taking into account the average void fraction and pressure drop of the mixture flow of a gas/non-Newtonian liquid. The pressure drop gradient model of Taitel and Barnea for a gas/Newtonian liquid slug flow was extended to include liquids possessing shear-thinning flow behaviour in inclined pipes. The comparison of the predicted values with the experimental data shows that the models presented here provide a reasonable estimate of the average void fraction and the corresponding pressure drop for the mixture flow of a gas/non-Newtonian liquid.

Keywords: Two-phase flow; Shear-thinning fluid; Flow pattern; Void fraction; Pressure drop; Inclination flow

1. Introduction

In recent years, considerable effort has been made to study simultaneous gas–liquid two-phase flows in horizontal and inclined pipes. The three most important hydrodynamic features of gas–liquid flows in engineering applications, which are the flow pattern, the void fraction, and the pressure drop of two-phase flows, have been studied experimentally and theoretically. In order to accurately estimate the pressure drop and void

* Corresponding author. Tel.: +86 10 6256 2770; fax: +86 10 6256 1284.
E-mail addresses: xujingyu@imech.ac.cn (J.-y. Xu), yxwu@imech.ac.cn (Y.-x. Wu).

0301-9322/$ - see front matter © 2007 Elsevier Ltd. All rights reserved.
doi:10.1016/j.ijmultiphaseflow.2007.03.008

fraction, it is necessary to know the actual flow pattern under specific flow conditions. A wide variety of flow patterns have been examined depending upon their physical properties and input fluxes of the two phases and the size and inclination of the pipe. So far, dozens of experimental investigations of flow pattern maps have been proposed in the literature for a gas/Newtonian fluid two-phase mixture in inclined pipes (Mukherjee, 1979; Spedding and Nguyen, 1980; Shoham, 1982; Kokal and Stanislav, 1989; Oddie et al., 2003). However, very little information is available for the case when the liquid phase is non-Newtonian, especially in inclined pipes. Recent works reporting data of flow pattern maps of gas/non-Newtonian liquid mixture flows are those of Chhabra and Richardson (1984) for horizontal flow and Khatib and Richardson (1984) and Dziubinski et al. (2004) for vertical flow. Chhabra and Richardson slightly modified the horizontal flow pattern map of Mandhane et al. (1974) on the basis of an analysis of the available data of the mixture flow of gas/shear-thinning liquids. Their results showed that the physical properties of the system had relatively little influence on horizontal flow regimes. However, except for the intermittent and annular flow, there was insufficient experimental data to verify the modified map of Chhabra and Richardson. Khatib and Richardson worked on suspensions of china clay in vertical upward flowing pipes and their results compared well with the predictions of boundaries between the various flow patterns, which were also largely unaffected by the rheology of the liquid. Dziubinski obtained data for tubes with diameters of 25.3–50.5 mm and lengths of 5 m and the map for the determination of flow patterns for two-phase flows of gas/non-Newtonian liquid in a vertical pipe were presented.

Following experimental studies, mechanistic modeling of the transitions between different flow patterns was started by Taitel. Although their work did not consider the calculation of pressure drop and void fraction, it was the pioneering work which considered physical mechanisms and opened the door for theoretical models of each flow pattern. Moreover, Barnea (1987) presented a unified model valid for the whole range of pipe inclination angles, which enabled various models to be linked together through unified flow pattern transition criteria. Following the work by Taitel and Barnea, comprehensive mechanistic models were presented by Xiao et al. (1990), Ansari et al. (1994), Kaya et al. (1999), Gomez et al. (2000), Petalas and Aziz (2000) and Zhang et al. (2003a,b). These models contain the determination of flow patterns and the computation of pressure drop and void fraction, but most of the models are for the case when the liquid phase exhibits Newtonian fluid behaviour. Very little work has been reported on inclined pipes with two-phase flows of gas/non-Newtonian liquid.

Unlike with the case of two-phase flow patterns, considerable interest has been shown in studying the flow properties of a gas/liquid mixture in a pipe when the liquid phase exhibits non-Newtonian fluid behaviour, including the two-phase void fraction (Oliver and Young-Hoon, 1968; Heywood and Charles, 1979; Farooqi and Richardson, 1982a; Chhabra and Richardson, 1986; Das et al., 1992; Johnson and White, 1993), and the two-phase pressure drop (Oliver and Young-Hoon, 1968; Mahalingam and Valle, 1972; Farooqi et al., 1980; Farooqi and Richardson, 1982b; Chhabra et al., 1983, 1984; Dziubinski, 1995; Kaminsky, 1998; Ruiz-Viera et al., 2006). These studies indicate, in general, that gas/non-Newtonian liquid two-phase flow hydrodynamics in pipes behave differently from the hydrodynamics of a gas/Newtonian liquid mixture flow, which are of great industrial importance in the transport of fluids and related operations. For example, a two-phase flow of gas/non-Newtonian liquid in a pipe enables a significant reduction in the average pressure gradient, which is of great practical importance in the transport of non-Newtonian liquid.

For the prediction of the average void fraction and pressure drop for the mixture flow of gas/non-Newtonian liquid one available method is of entirely empirical nature. Farooqi and Richardson (1982) modified the Lockhart and Martinelli (1949) model to predict the average void fraction and studied the drag reduction phenomenon in the intermittent regime. Dziubinski (1995) developed a general expression of drag ratio for two-phase pressure drop during an intermittent flow of gas/non-Newtonian liquid based on the concept of loss coefficient. In addiction to these, Ruiz-Viera et al. (2006) experimentally observed the mixture flows of air/lubricating grease using different geometries with both smooth and rough surfaces, and introduced an empirical model for the two-phase pressure drop with a combination of power-law and sigmoidal-type equations. These methods need little information about two-phase flow structures, so they are easy to solve for the void fraction and pressure drop of two-phase flows. However, these methods are entirely empirical in nature, and therefore the extrapolation beyond the range of experimental conditions must be treated with reserve.

Another method is based on models which utilize information that is implicit in the flow pattern. Unfortunately, there are very few studies with this method for a mixture flow of gas/non-Newtonian liquid due to its complexity. Heywood and Charles (1979) extended the model of gas/Newtonian liquid flow formulated by Taitel and Dukler (1976), which was not tested against data, for predicting the liquid holdup and pressure drop of gas/non-Newtonian liquid in a unified stratified flow. Eisenberg and Weinberger (1979) used similar idealized models to calculate the annular flow of gas/power-law liquids in horizontal pipes. But these studies are only for stratified and annular flows in horizontal pipes, and there are few available methods that studied other flow patterns of gas/non-Newtonian liquid, especially for inclined flows.

The gas/non-Newtonian liquid two-phase flow in inclined pipes occurs in a wide range of practical applications in the chemical, oil and process industries. For example, in the petroleum industry a gas/non-Newtonian fluid flow often occurs in hilly terrain pipelines, downcomer pipes extending from offshore production platforms to sea floors, and steam injection wells in thermally enhanced recovery operations. Therefore, the objective of this work is to carry out systematic experimental and theoretical studies on two-phase co-current flow characteristics in inclined pipes including two-phase flow patterns, void fraction and pressure drop, especially for the mixture flow of gas/non-Newtonian liquid.

In what follows, Section 2 gives a detailed description of the experimental setup. Then the test matrix and the theoretical models are presented in Sections 3 and 4 respectively. In Section 5 the measurement data is presented, and the results of the prediction of void fraction and pressure drop of a gas/non-Newtonian fluid flow are compared with the measurements and are discussed. The paper closes with a summary of the main conclusions in Section 6.

2. Experimental setup and fluid characteristics

2.1. Flow loop and procedure

The experimental investigations were conducted using the setup shown in Fig. 1. Air originates from a compressor pump and is routed through a gas tank and a regulating valve to maintain a constant pressure, after which it passes through a gas mass flowmeter. The liquid phase is conveyed from the liquid phase tank and circulated through the system by a centrifugal pump. The liquid phase and the gas phase are fed into the pipeline via a T-junction. The volumetric flow rates of all phases can be regulated independently and are measured by a thermal mass flowmeter for the gas phase and an electromagnetic flowmeter for the liquid phase.

The multiphase flow pipeline is constructed using Perspex tubing of 20, 40 and 60 mm in diameter. Each tube includes two 10 m long pipe branches connected by a U-bend that can be inclined to any angle, from a completely horizontal to a fully vertical position. With this installation experiments on upward and downward flows can be carried out simultaneously. When the installation is slanted to $+5°$ from the horizontal, the downward flow in the return branch pipes is at an angle of $-5°$. Inclination angles reported in this work are accurate to $\pm 0.05°$. Three ball valves are used to control the flow in the test section, shown as No. 12 in Fig. 1. For instance, in one experiment the valve fixed on the 60 mm diameter pipe is opened and other valves are closed. The two-phase mixture passes through the 60 mm diameter test section where the data is collected and then flows down the return line into the liquid tank. Flow pattern, void fraction and pressure drop are investigated.

Flow patterns are recorded using a high-speed video camera, and the flow patterns for each test condition are recorded and can be observed later in slow motion. Pressure drop in the test section is measured by two absolute pressure transducers, and accurate results can be obtained from the difference of the measurements between the two transducers which are located at both ends of the 6 m long straight test section. The sampling frequency of the pressure is 500 Hz and a total of 150,000 samples, which corresponds to 5 min sampling time, are collected. Void fraction is estimated at the midpoint of the 60 mm diameter test section using gamma-ray absorption technique. The gamma densitometer was installed at 5 m from the entry point. This provides sufficient entrance length to stabilize the flow. The gamma densitometer measures gamma ray absorption which allows the mean void fraction in the pipe to be calculated. During the measurement the device is aligned perpendicular to the flow with a ^{137}Cs source on the bottom half of the pipe and the detector with an 8 mm diameter collimator on the top as is shown in Fig. 2. The gamma ray densitometer is calibrated by scanning a

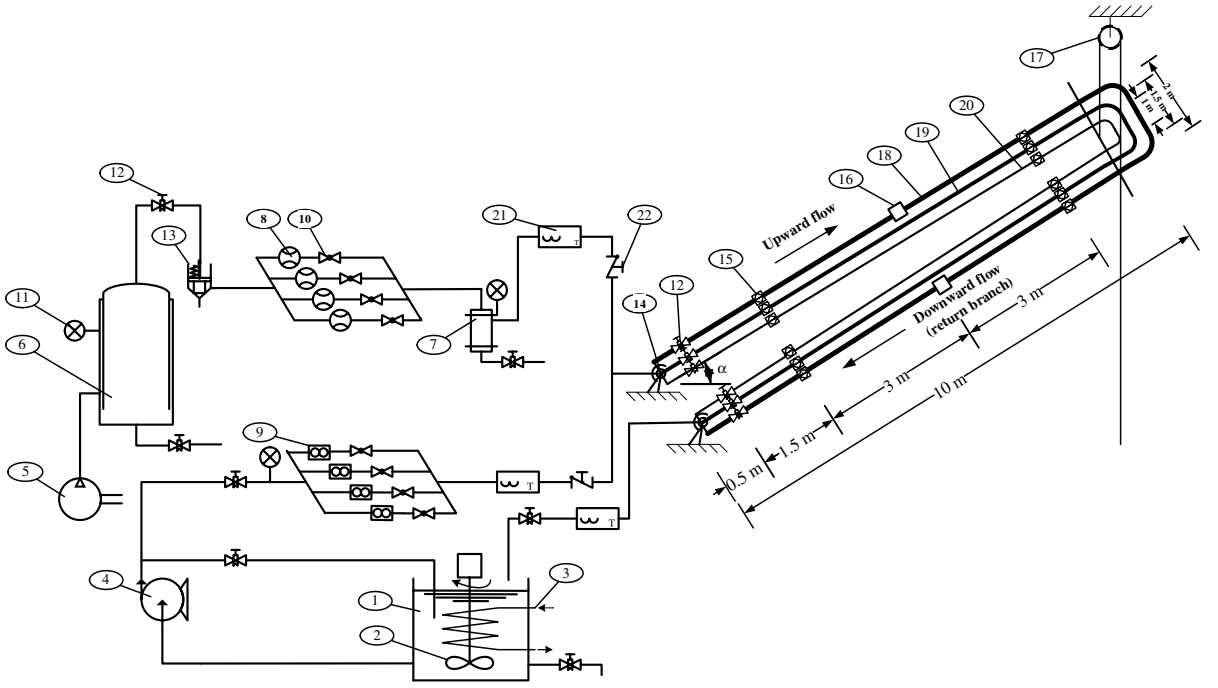

Fig. 1. Schematic of the test facility. 1 – liquid tank, 2 – blender, 3 – coils, 4 – centrifugal pump, 5 – air compressor, 6 – gas tank, 7 – water trap, 8 – thermal mass flowmeter, 9 – electromagnetic flowmeter, 10 – electromagnetic valve, 11 – pressure gauge, 12 – control valves, 13 – regulating valve, 14 – gear wheel, 15 – pressure drop measuring sensor, 16 – gamma densitometer, 17 – block and tackle, 18 – 60 mm ID test section, 19 – 40 mm ID test section and 20 – 20 mm ID test section.

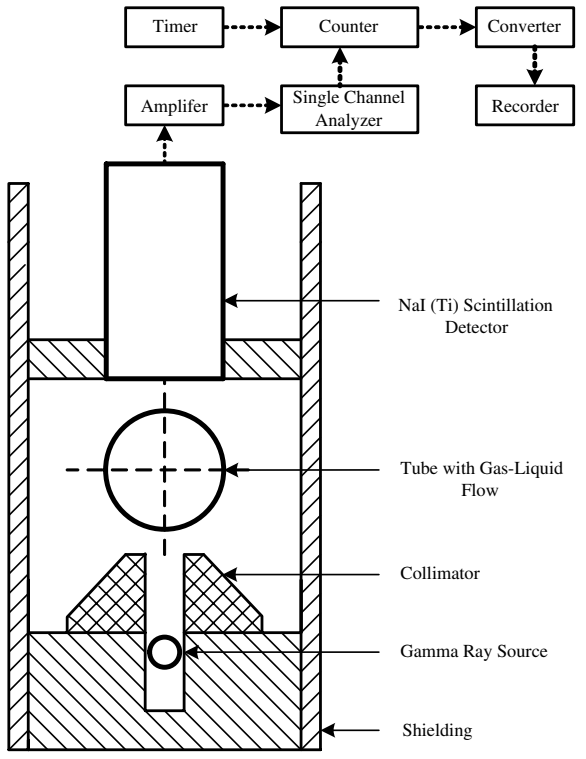

Fig. 2. Schematic of the gamma-densitometer.

Table 1
The physical properties of the liquid phase measured at 20 °C and 0.101 MPa

Liquid phase	Concentration (kg/m)	Density, ρ (kg/m^3)	Surface tension, σ (N/m)	Fluid consistency coefficient, m_0 (Pa s^{n0})	Flow behaviour index, n_0
Water	–	999.0	0.0712	0.001	1.000
CMC-1 solution	1.0	999.9	0.0714	0.089	0.798
CMC-2 solution	2.0	1000.0	0.0718	0.469	0.658
CMC-3 solution	3.0	1000.4	0.0727	0.972	0.615

Plexiglass box which contains several water to gas ratios and thus gives different void fraction values to be used as calibration points. The counting rate is integrated over 80 energy bands centered at the peak energy band of the 662 keV value generated from the ^{137}Cs scattering. The test section was scanned for 5 separate periods of 60 s to obtain an average value of void fraction. Furthermore, due to the effect that different flow patterns have on the measurement, the experimental data has been further amended using the method proposed by Stahl and Rudolf von Rohr (2004).

2.2. Fluid characteristics

Tap water is used as the Newtonian liquid phase and CMC (carboxymethyl cellulose) solutions with three different concentrations are used as the non-Newtonian liquid phases. These are prepared by adding small quantities of dry polymer powders which are gently stirred to prevent the formation of lumps. The density of each solution was measured using a constant volume density bottle. The CMC rheology experiments are measured with a ThermoHaake RS300 rheometer. A double gap cylinder sensor system with an outside gap of 0.30 mm and an inside gap of 0.25 mm is used for this purpose.

As expected, CMC solutions in this study are shear-thinning fluids whose rheology can be described by a two-parameter power-law fluid model. For a power-law fluid, the shear stress is related to the shear rate by Chhabra and Richardson (1999)

$$\tau = m_0(\dot{\gamma})^{n_0} \tag{1}$$

where $\dot{\gamma}$ is the shear rate. m_0 and n_0 are two empirical curve-fitting parameter and are known as the fluid consistency coefficient and the flow behaviour index, respectively. The values of m_0, n_0 and other properties of the CMC solutions are given in Table 1.

3. Test matrix

Since most reported studies focus on horizontal and vertical pipes, the present work carries out several series of tests in pipelines with inclination angles from −75° to +75°. To collect the maximum amount of data on gas–liquid two-phase flow in inclined pipes and study the effects of pipe diameter and inclination on the flow pattern, void fraction and pressure drop, the experiments cover a wide range of flow rates for different CMC solutions at diverse angle and with a number of flow patterns. Table 2 shows the experimental test matrix for tests carried out on the two-phase flow system. A total of 800 experimental tests were conducted.

Table 2
Experimental test matrix

Diameter	Superficial velocities	Experimental system	Pipe inclination
20 mm	$0.78 < U_{LS} < 1.82$	Air/water	0°, ±15°
	$0 < U_{GS} < 13.54$	Air/all three different CMC solutions	
40 mm	$0.51 < U_{LS} < 2.03$	Air/water	0°, ±15°
	$0 < U_{GS} < 4.82$	Air/all three different CMC solutions	
60 mm	$0.5 < U_{LS} < 1.84$	Air/water	0°, ±5°, ± 15°,
	$0 < U_{GS} < 3.52$	Air/all three different CMC solutions	±30°, ±75°

4. Theoretical considerations

4.1. Two-phase flow patterns

The methods available for predicting flow patterns are mostly suitable for Newtonian liquids. In contrast, very little information for gas/non-Newtonian liquid flow is available. Thus, in this work we attempt to extend existing flow pattern maps to include shear-thinning materials in accordance with a unified model presented by Barnea (1987). This model developed from the analysis of physical transition mechanisms modeled by fundamental equations.

4.2. Void fraction and pressure drop for the gas/non-Newtonian fluid flow

For inclined flows the most prominent feature is a preponderance of a stratified flow pattern in the downward inclined pipe and a preponderance of an intermittent flow pattern in upward inclined pipe (Hetsroni, 1982). Therefore, in this work, studies of the void fraction and pressure drop focus on stratified flows and intermittent flows for a gas/non-Newtonian fluid flow. Due to the high viscosity of the liquid phase, for the stratified flow the liquid phase is treated as a laminar flow to calculate the void fraction and the two-phase pressure drop. For the intermittent flow, we treated the liquid phase as a laminar flow in the film zone to render the equations dimensionless and for simplification. In the liquid slug zone we treated the mixture flow as a laminar or turbulent flow, depending upon the Reynolds number, to calculate the pressure drop.

4.2.1. Stratified flow

The model for stratified flow is derived by Taitel and Dukler (1976) for gas/Newtonian liquid flow and extended by Heywood and Charles (1979) for gas/non-Newtonian liquid horizontal flow as illustrated in Fig. 3. The flow is assumed to be one-dimensional and stratified along the length of the pipe, which can be inclined from a horizontal position up to a vertical position. Ignoring the effects of acceleration and hydraulic gradient in the liquid phase, the momentum balance for the liquid and gas phase is written as follows:

$$-A_{\mathrm{L}}\left(\frac{\mathrm{d}p}{\mathrm{d}x}\right)_{\mathrm{TP}} - \tau_{\mathrm{L}}S_{\mathrm{L}} + \tau_{\mathrm{i}}S_{\mathrm{i}} - \rho_{\mathrm{L}}A_{\mathrm{L}}g\sin\alpha = 0 \tag{2}$$

$$-A_{\mathrm{G}}\left(\frac{\mathrm{d}p}{\mathrm{d}x}\right)_{\mathrm{TP}} - \tau_{\mathrm{G}}S_{\mathrm{G}} - \tau_{\mathrm{i}}S_{\mathrm{i}} - \rho_{\mathrm{G}}A_{\mathrm{G}}g\sin\alpha = 0 \tag{3}$$

where A is area, S is wetted periphery, τ is the shear stress and ρ is the density. The subscripts TP, G, L and i refer to the two-phase, gas phase, liquid phase and interface, respectively, α is the angle of inclination from the horizontal and g is the acceleration due to gravity. Eliminating the pressure gradient, $\mathrm{d}p/\mathrm{d}x$, from Eqs. (2) and (3) gives

$$\tau_{\mathrm{G}}\frac{S_{\mathrm{G}}}{A_{\mathrm{G}}} - \tau_{\mathrm{L}}\frac{S_{\mathrm{L}}}{A_{\mathrm{L}}} + \tau_{\mathrm{i}}S_{\mathrm{i}}\left(\frac{1}{A_{\mathrm{L}}} + \frac{1}{A_{\mathrm{G}}}\right) - (\rho_{\mathrm{L}} - \rho_{\mathrm{G}})g\sin\alpha = 0 \tag{4}$$

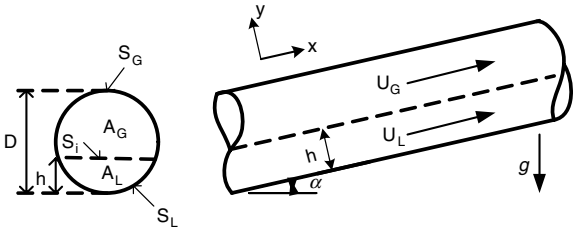

Fig. 3. Illustration of geometry of the idealized stratified flow in a round pipe.

The shear stresses are defined by

$$\tau_G = f_G \frac{\rho_G U_G^2}{2}; \quad \tau_L = f_L \frac{\rho_L U_L^2}{2}; \quad \tau_i = f_i \frac{\rho_G (U_G - U_L)|U_G - U_L|}{2} \tag{5}$$

where U is the average velocity of each phase. The liquid and gas friction factors in a smooth pipe can be approximated by

$$f_L = C_L \cdot Re_L^{-n}; \quad f_G = C_G \cdot Re_G^{-m} \tag{6}$$

where $C_L = C_G = 0.046$, $n = m = 0.2$ for turbulent flow, and $C_L = C_G = 16$, $n = m = 1$ for laminar flow. The Reynolds number for the gas phase as Newtonian fluid is defined by

$$Re_G = \frac{D_G U_G \rho_G}{\mu_G}, \quad D_G = \frac{4A_G}{S_G + S_i} \tag{7}$$

For non-Newtonian materials the rheological behaviour obeys Eq. (1). The appropriate Reynolds number is defined as

$$Re_{MR} = \frac{D_L^{n_0} U_L^{2-n_0} \rho_L}{8^{n_0-1} m_0 \left(\frac{1+3n_0}{4n_0}\right)^{n_0}}, \quad D_L = \frac{4A_L}{S_L} \tag{8}$$

where μ is the viscosity, D_G and D_L are the equivalent diameters for the gas and liquid phases, respectively. For the interfacial gas–liquid shear stress, we use a constant value $f_i = 0.014$ (Cohen and Hanratty, 1968). By designating the dimensionless quantities with a tilde (~), substitution of Eqs. (5)–(8) into (4) leads to

$$X^2 \cdot \left(\frac{\tilde{S}_L \cdot \tilde{U}_L^{n_0}}{\tilde{A}_L \cdot \tilde{D}_L^{n_0}}\right) - \frac{\tilde{S}_G \cdot \tilde{U}_G^{2-m}}{\tilde{A}_G \cdot \tilde{D}_G^{m}} - \frac{f_i}{f_G} \cdot \frac{\tilde{U}_G^{2-m}}{\tilde{D}_G^{m}} \cdot \left(1 - q \cdot \frac{\tilde{U}_L}{\tilde{U}_G}\right) \cdot \left|1 - q \cdot \frac{\tilde{U}_L}{\tilde{U}_G}\right| \cdot \left(\frac{\tilde{S}_i}{\tilde{A}_L} + \frac{\tilde{S}_i}{\tilde{A}_G}\right) - 4Y = 0 \tag{9}$$

where $q = U_{SL}/U_{SG}$; $\tilde{U}_L = U_L/U_{SL}$ and $\tilde{U}_G = U_G/U_{SG}$; $\tilde{D}_L = D_L/D$ and $\tilde{D}_G = D_G/D$; $\tilde{S}_L = S_L/D$, $\tilde{S}_G = S_G/D$ and $\tilde{S}_i = S_i/D$; $\tilde{A}_L = A_L/D^2$ and $\tilde{A}_G = A_G/D^2$. X^2 is the Lockhart and Martinelli (1949) parameter defined as

$$X^2 = \frac{(dp_F/dx)_{SL}}{(dp_F/dx)_{SG}} \tag{10}$$

where the subscript F refers to the frictional pressure gradient, the subscripts SG and SL refer to superficial gas and liquid phase for either phase flowing alone in the channel, respectively. Y is a parameter defined by Taitel and Dukler (1976) to represent the effect of channel inclination as follows:

$$Y = \frac{-(\rho_L - \rho_G) g \sin\alpha}{(dp_F/dx)_{SG}} \tag{11}$$

All the dimensionless pressure quantities with a tilde (~) are functions of the dimensionless liquid height, $\tilde{h}_L = h_L/D$. $\tilde{h}_L$ can be solved numerically by implicit Eq. (9). If $\tilde{h}_L$ is estimated, the void fraction, ε, may be calculated as follows:

$$\varepsilon = \frac{1}{\pi}\left[\cos^{-1}(2\tilde{h}_L - 1) - (2\tilde{h}_L - 1)\sqrt{1 - (2\tilde{h}_L - 1)^2}\right] \tag{12}$$

Once a solution has been obtained for the void fraction, the corresponding pressure drop can be calculated by the sum of Eqs. (2) and (3). The total pressure drop is composed of the gravitational pressure drop and the frictional pressure gradient, which can be determined by the void fraction. The dimensionless pressure drop is given by

$$\Phi_G^2 = \frac{(dp/dx)_{TP}}{(dp_F/dx)_{SG}} = \frac{1}{\pi} \cdot \left(\tilde{S}_L \cdot X^2 \cdot \frac{\tilde{U}_L^{n_0}}{\tilde{D}_L^{n_0}} + \tilde{S}_G \cdot \frac{\tilde{U}_G^{2-m}}{\tilde{D}_G^{m}}\right) - Y \cdot \frac{[\rho_L \cdot \tilde{A}_L + \rho_G \cdot \tilde{A}_G]}{(\tilde{A}_L + \tilde{A}_G)(\rho_L - \rho_G)} \tag{13}$$

where Φ_G^2 is the Lockhart–Matinelli multiplier parameter. And since, by definition

$$\Phi_L^2 = \frac{(dp/dx)_{TP}}{(dp_F/dx)_{SL}} = \frac{\Phi_G^2}{X^2} \tag{14}$$

Substituting of Eq. (14) into (13) leads to

$$\Phi_{\mathrm{L}}^2=\frac{(\mathrm{d}p/\mathrm{d}x)_{\mathrm{TP}}}{(\mathrm{d}p_{\mathrm{F}}/\mathrm{d}x)_{\mathrm{SL}}}=\frac{1}{\pi}\cdot\left(\tilde{S}_{\mathrm{L}}\cdot\frac{\tilde{U}_{\mathrm{L}}^{n_0}}{\tilde{D}_{\mathrm{L}}^{n_0}}+\tilde{S}_{\mathrm{G}}\cdot\frac{1}{X^2}\frac{\tilde{U}_{\mathrm{G}}^{2-m}}{\tilde{D}_{\mathrm{G}}^{m}}\right)-\frac{Y}{X^2}\cdot\frac{[\rho_{\mathrm{L}}\cdot\tilde{A}_{\mathrm{L}}+\rho_{\mathrm{G}}\cdot\tilde{A}_{\mathrm{G}}]}{(\tilde{A}_{\mathrm{L}}+\tilde{A}_{\mathrm{G}})(\rho_{\mathrm{L}}-\rho_{\mathrm{G}})} \tag{15}$$

For horizontal flow, the dimensionless frictional pressure gradient, Φ_{F}^2 can be expressed as

$$\Phi_{\mathrm{F}}^2=\frac{1}{\pi}\cdot\left(\tilde{S}_{\mathrm{L}}\cdot\frac{\tilde{U}_{\mathrm{L}}^{n_0}}{\tilde{D}_{\mathrm{L}}^{n_0}}+\tilde{S}_{\mathrm{G}}\cdot\frac{1}{X^2}\frac{\tilde{U}_{\mathrm{G}}^{2-m}}{\tilde{D}_{\mathrm{G}}^{m}}\right) \tag{16}$$

Then the drag reduction occurs in stratified flow

$$\tilde{S}_{\mathrm{L}}\cdot\frac{\tilde{U}_{\mathrm{L}}^{n_0}}{\tilde{D}_{\mathrm{L}}^{n_0}}+\tilde{S}_{\mathrm{G}}\cdot\frac{1}{X^2}\frac{\tilde{U}_{\mathrm{G}}^{2-m}}{\tilde{D}_{\mathrm{G}}^{m}}<4(\tilde{A}_{\mathrm{L}}+\tilde{A}_{\mathrm{G}})=\pi \tag{17}$$

If ε is known, this criterion may be used to determine whether drag reduction exists in stratified gas/non-Newtonian liquid flow by solving Eq. (17).

4.2.2. Intermittent flow

Each slug unit of length L_{U} is composed of two separate sections: the liquid slug zone of length L_{S} and the film zone of length L_{L} as shown in Fig. 4. The mechanistic model used for steady slug flow was studied in detail by Taitel and Barnea (1990). Assuming that the film contains no entrained gas bubbles and both the liquid and gas are incompressible, the liquid and gas mass balances over the slug unit yielding:

$$U_{\mathrm{SL}}=\frac{1}{L_{\mathrm{U}}}\cdot\left[(1-\varepsilon_{\mathrm{S}})\cdot L_{\mathrm{S}}\cdot U_{\mathrm{S}}+\int_0^{L_{\mathrm{L}}}U_{\mathrm{L}}\cdot(1-\varepsilon_{\mathrm{L}})\cdot\mathrm{d}x\right] \tag{18}$$

$$U_{\mathrm{SG}}=\frac{1}{L_{\mathrm{U}}}\cdot\left[\varepsilon_{\mathrm{S}}\cdot L_{\mathrm{S}}\cdot U_{\mathrm{S}}+\int_0^{L_{\mathrm{L}}}U_{\mathrm{G}}\cdot\varepsilon_{\mathrm{L}}\cdot\mathrm{d}x\right] \tag{19}$$

where ε is the void fraction, the subscripts S and L refer to the liquid slug and elongated bubble zone, respectively. U_{G} is the elongated gas bubble velocity. Following Taitel and Barnea (1990), the aerated liquid slug velocity, U_{S} is evaluated by

$$U_{\mathrm{S}}=U_{\mathrm{M}}=U_{\mathrm{SL}}+U_{\mathrm{SG}} \tag{20}$$

where U_{M} is the mixture velocity of the superficial gas and liquid phase. A gas mass balance relative to a coordinate system that moves with a translation velocity, U_{T} yields

$$\varepsilon_{\mathrm{L}}\cdot(U_{\mathrm{T}}-U_{\mathrm{G}})=\varepsilon_{\mathrm{S}}\cdot(U_{\mathrm{T}}-U_{\mathrm{S}}),\quad U_{\mathrm{T}}=C\cdot U_{\mathrm{M}}+U_{\mathrm{D}} \tag{21}$$

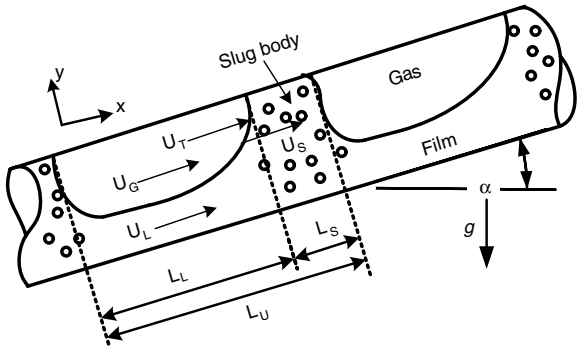

Fig. 4. Illustration of the geometry of slug flow in a round pipe.

where C is related to the liquid velocity profile ahead of the elongated bubble, using $C = 1.2$ for turbulent flow and $C = 2.0$ for laminar flow. U_D is the drift velocity. For horizontal and upward inclined pipe flows, following Bendiksen (1984) proposition

$$U_D = 0.35 \cdot \sqrt{g \cdot D} \cdot \sin\alpha + 0.54\sqrt{g \cdot D} \cdot \cos\alpha \tag{22}$$

The volume average void fraction, ε, over a slug unit is

$$\varepsilon = \frac{\varepsilon_S \cdot L_S + \int_0^{L_L} \varepsilon_L \cdot dx}{L_U} \tag{23}$$

Using Eq. (23) to eliminate the integral term in Eq. (19) yields

$$\varepsilon = \frac{1}{U_T} \cdot (U_{SG} - \varepsilon_S \cdot U_M) + \varepsilon_S \tag{24}$$

where the void fraction within the liquid slug, ε_S, following the recommendation offered by Gregory et al. (1978) is

$$\varepsilon_S = 1 - \frac{1}{1 + (U_M/8.66)^{1.39}} \tag{25}$$

Assuming a uniform film along the film zones, the average pressure gradient in a slug unit is obtained by performing a momentum balance over a global control volume of the slug unit, one obtains

$$\left(\frac{dp}{dx}\right)_{TP} = \rho_U g \sin\alpha + 2\frac{f_S}{D}\rho_S U_S^2 \frac{L_S}{L_U} + \frac{4}{\pi \cdot D^2} \cdot \frac{L_L}{L_U}\left(\frac{f_G \rho_G U_G^2}{2} S_G + \frac{f_L \rho_L U_L^2}{2} S_L\right) \tag{26}$$

where $\rho_U = \varepsilon \cdot \rho_G + (1-\varepsilon)\rho_L$ is the average density over a slug unit, $\rho_S = \varepsilon_S \rho_G + (1-\varepsilon_S)\rho_L$ is the average density within the liquid slug, and f_S is the liquid slug friction factor, which is calculated in the same way as f_L with the liquid slug Reynolds number given by

$$Re_S = \frac{D^{n_0} U_S^{2-n_0} \rho_S}{8^{n_0-1} m_0 \left(\frac{1+3n_0}{4n_0}\right)^{n_0}} \tag{27}$$

The other parameters in Eq. (27) can be expressed in terms of the parameters mentioned above.

Once a solution has been obtained for the void fraction, ε_L, in the elongated bubble zone and the average gas velocity, U_G, by solving Eq. (4) numerically, the total pressure drop can be solved by substituting Eqs. (18)–(24) into (26). With non-dimensional quantities denoted by a tilde (~), Eq. (26) reduces to

$$\Phi_G^2 = \frac{(dp/dx)_{TP}}{(dp_F/dx)_{SG}} = -Y \cdot \frac{\rho_U}{(\rho_L - \rho_G)} + Z^2 \cdot \frac{L_S}{L_U} + \frac{1}{\pi} \cdot \frac{L_L}{L_U}\left(\tilde{S}_L \cdot X^2 \cdot \frac{\tilde{U}_L^{n_0}}{\tilde{D}_L^{n_0}} + \tilde{S}_G \cdot \frac{\tilde{U}_G^{2-m}}{\tilde{D}_G^{m}}\right) \tag{28}$$

where

$$Z^2 = \frac{(dp_F/dx)_S}{(dp_F/dx)_{SG}} = \frac{2\frac{f_S \rho_S U_S^2}{D}}{2\frac{f_G \rho_G U_G^2}{D}} \tag{29}$$

For horizontal flow the dimensionless frictional pressure gradient can be given by

$$\Phi_F^2 = \frac{(dp/dx)_{TP}}{(dp_F/dx)_{SL}} = Z^2 \cdot \frac{L_S}{L_U} \cdot \frac{1}{X^2} + \frac{1}{\pi} \cdot \frac{L_L}{L_U}\left(\tilde{S}_L \cdot \frac{\tilde{U}_L^{n_0}}{\tilde{D}_L^{n_0}} + \tilde{S}_G \cdot \frac{\tilde{U}_G^{2-m}}{\tilde{D}_G^{m}} \cdot \frac{1}{X^2}\right) \tag{30}$$

For gas/non-Newtonian two-phase flow in horizontal pipe, Eq. (30) is also the equation for the drag ratio. Thus, the drag reduction occurs, when

$$Z^2 \cdot \frac{L_S}{L_U} \cdot \frac{\pi}{X^2} + \frac{L_L}{L_U}\left(\tilde{S}_L \cdot \frac{\tilde{U}_L^{n_0}}{\tilde{D}_L^{n_0}} + \tilde{S}_G \cdot \frac{\tilde{U}_G^{2-m}}{\tilde{D}_G^{m}} \cdot \frac{1}{X^2}\right) < \pi \tag{31}$$

If L_S/L_U, L_L/L_U, Z and $\tilde{h}_L$ are known, Eq. (31) may be used to determine whether drag reduction exists in intermittent gas/non-Newtonian liquid flow.

5. Results and discussion

The experimental results are presented for two-phase flow patterns, void fraction and two-phase pressure drop, which are compared against data available in the published literature. The developed mechanistic models for gas/non-Newtonian fluid flow were verified with experimental results.

5.1. Two-phase flow patterns

The designation of flow patterns have been largely based on individual interpretation of visual observations. In this work the flow pattern definitions for gas/non-Newtonian liquid flows are also described according to gas/Newtonian liquid flow pattern definitions, although there are some differences between gas/Newtonian liquid and gas/non-Newtonian liquid flows for the same flow pattern. For instance there are fewer distinctly dispersed bubbles within a liquid slug for gas/non-Newtonian liquid flows than in those within a Newtonian liquid slug. Thus, in the present work the flow structures of gas/non-Newtonian fluid are

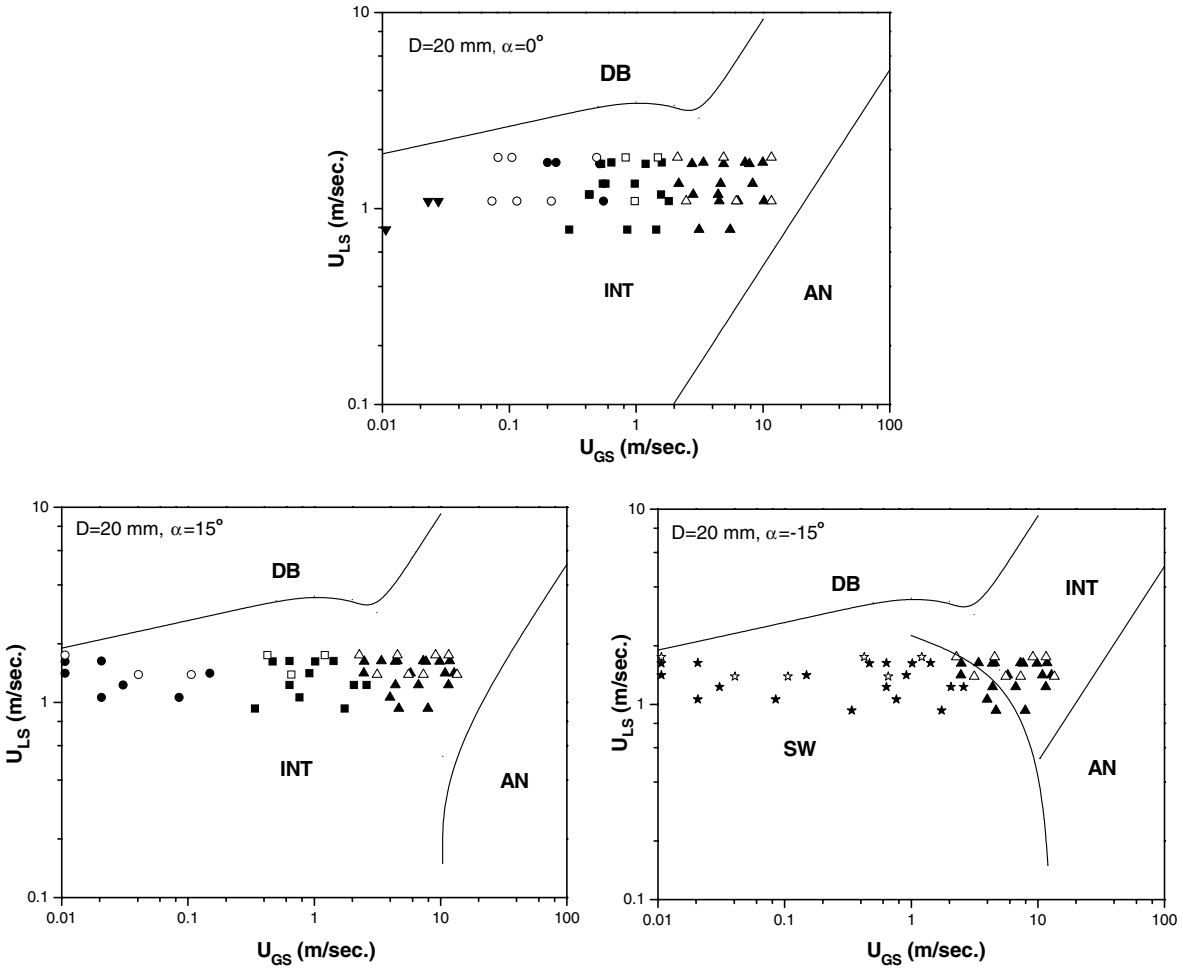

Fig. 5. Flow pattern map for inclined flow, $D = 20$ mm : –, theoretical line by Barnea (1987). Air-water systems: plug (○), slug (□), churn (△), stratified (☆), bubble (▽); air-CMC solutions systems: plug (●), slug (■), churn (▲), stratified (★), bubble (▼).

distinguished, in general, as six basic flow structures. They are: dispersed bubble, stratified (smooth or wavy), plug, slug, churn (or froth) and annular flow patterns.

Over the extent of pipe inclination angles and flow rates considered here, bubble, plug, slug, stratified, churn and annular flow patterns were observed. The results of these experiments were compared with the theoretical maps presented by Barnea (1987) in tubes of 20, 40 and 60 mm in diameter as shown in Figs. 5–7. It is shown that for gas/non-Newtonian liquid flow, the theoretical model can satisfactorily describe our experimental data for shallow inclinations (−30 to +30° inclinations in this work). However, this theoretical model failed to describe the position of the bubbly-intermittent boundary for steep inclinations (±75° inclinations in this work) as is shown in Fig. 7. The main differences are that the transition from bubbly to plug took place under a much lower contribution of the gas phase in the gas/non-Newtonian liquid flow than those in the gas/Newtonian liquid flow. Similar results were also found by Dziubinski et al. (2004) in vertical upward flows for gas/non-Newtonian liquid flows. The reasons for the discrepancies may be that the theoretical model is based on the properties of Newtonian liquids, not on those of non-Newtonian liquids. Moreover, we observed similar results with gas/non-Newtonian liquid flows as with gas/Newtonian liquid flow on the transition from slug to churn in a horizontal flow when the tube diameter is changed, as illustrated in Figs. 5 and 6.

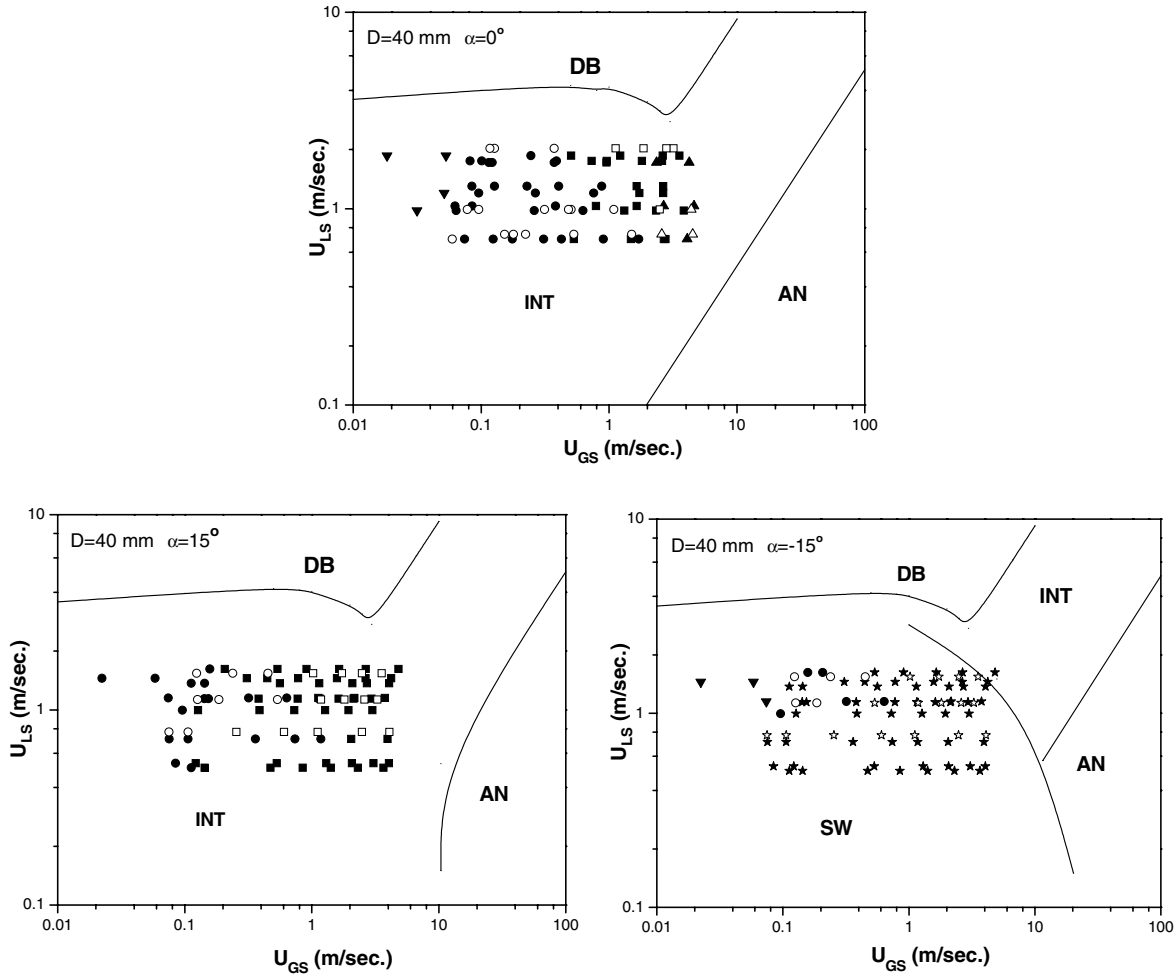

Fig. 6. Flow pattern map for inclined flow, $D = 40$ mm: –, theoretical line by Barnea (1987). Air-water systems : plug (○), slug (□), churn (△), stratified (☆), bubble (▽); air-CMC solutions systems: plug (●), slug (■), churn (▲), stratified (★), bubble (▼).

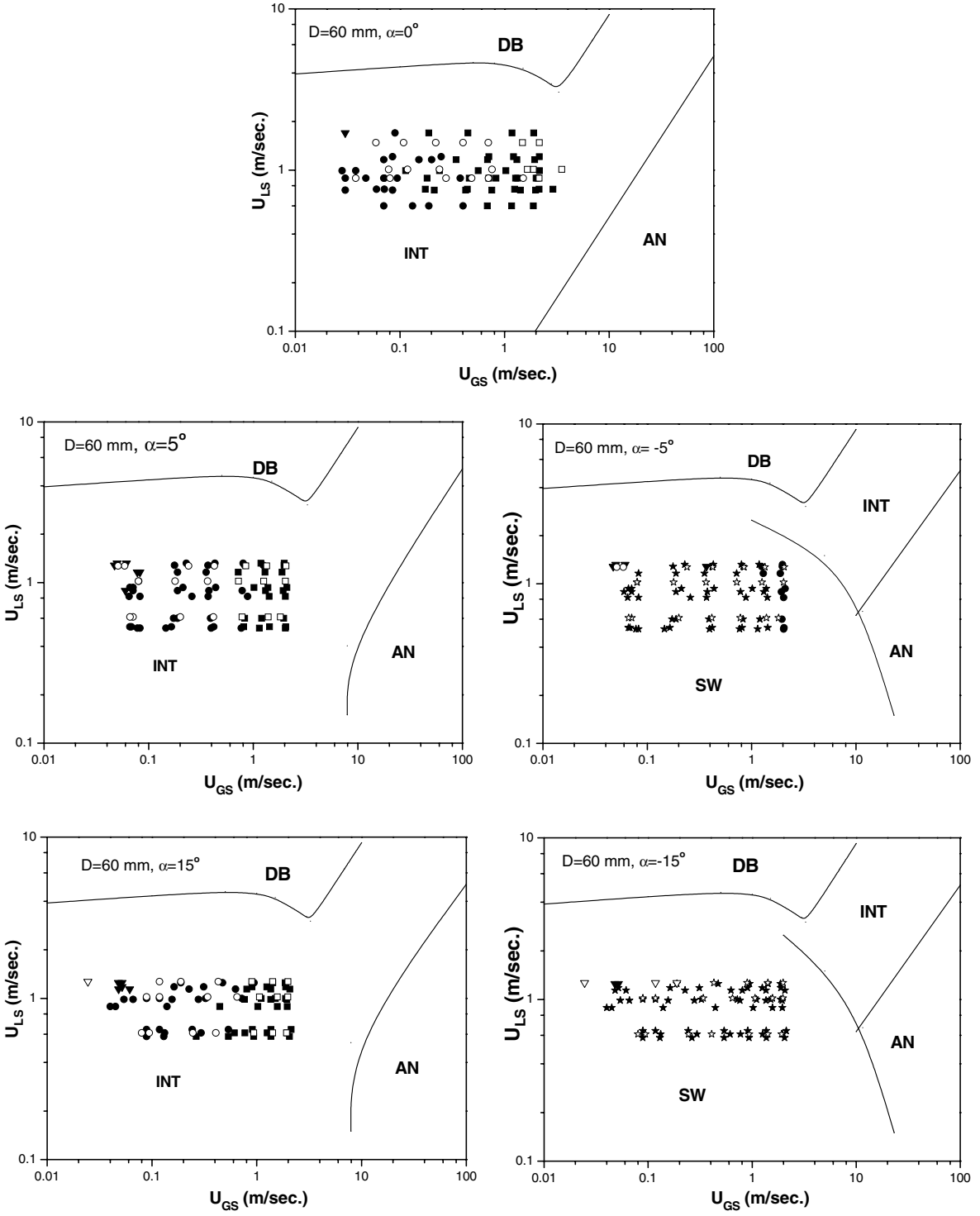

Fig. 7. Flow pattern map for the whole range of pipe inclinations, $D = 60$ mm pipes: –, theoretical line by Barnea (1987). Air–water systems: plug (○), slug (□), churn (△), stratified (☆), bubble (▽), annular (◇); air-CMC solutions systems: plug (●), slug (■), churn (▲), stratified (★), bubble (▼), annular (◆).

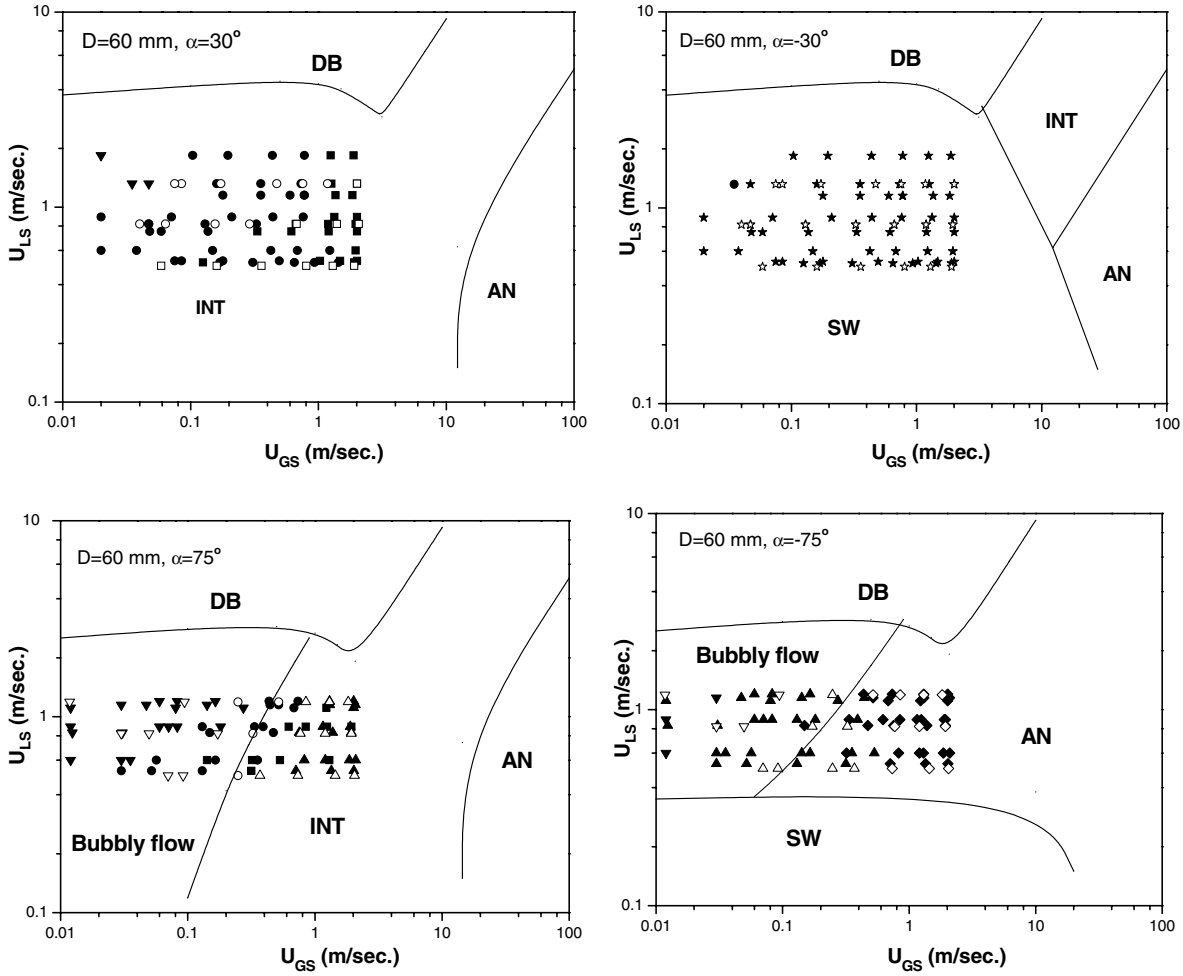

Fig. 7 (*continued*)

5.2. Void fraction

In the present work the void fraction was studied in the 60 mm diameter pipe using horizontal and inclined flows.

5.2.1. Stratified flow

As mentioned above, the void fraction can be numerically solved by the implicit Eq. (9) for gas/non-Newtonian liquid stratified flows in an inclined pipe. Due to the detailed studies on the in-situ volume fraction for gas/Newtonian liquid stratified flow that have been given by Taitel and Dukler (1976) and Ullmann et al. (2003b), the present investigation focuses on gas/non-Newtonian liquid stratified flows.

Fig. 8 shows the void fraction for power-law liquids as a function of the Lockhart–Martinelli parameter, X^2, in stratified flows for various n_0 values corresponding to shear-shinning fluid behaviour as predicted from Eq. (9). Over the range $0 \leqslant X^2 \leqslant 1000$, ε decreases for a given X^2 as n_0 is increased from 0.25 to 1.0. However, the reverse is true for all $X^2 < 0$ and such behaviour can occur in counter-current flows. Moreover, Fig. 8 also illustrates that in the range of relatively high X^2 values the effect of n_0 values on ε is of minor importance in a laminar-liquid and a turbulent-gas flow, although it will undoubtedly be an influence on the smooth or wavy interface that forms between the phases. Fig. 9 shows the effect of the pipe inclination parameter, Y, on the void fraction in stratified horizontal and inclined flows for gas/non-Newtonian liquid flows. Here co-current

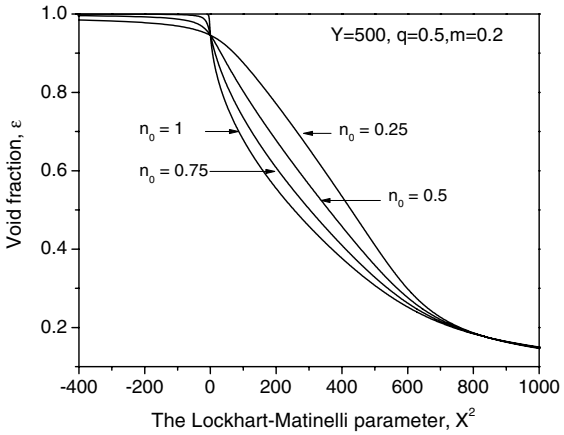

Fig. 8. The void fraction for power-law liquids as a function of the Lockhart–Martinelli parameter, X^2 in stratified downward flow.

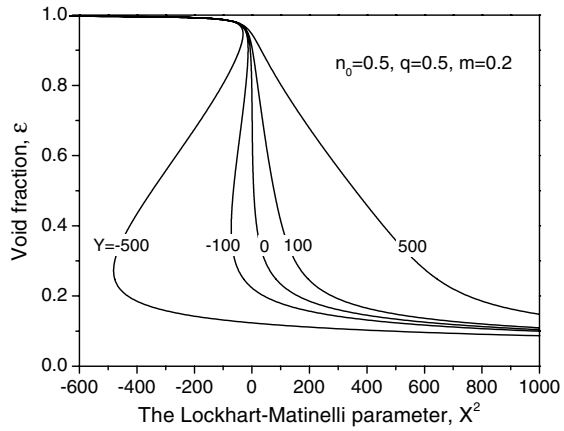

Fig. 9. The effect of the channel inclination parameter, Y on the void fraction in stratified horizontal and inclined flows ($Y > 0$, downward flow; $Y < 0$, upward flow).

flow corresponds to a positive X^2 with $Y < 0$ for the upward flow and $Y > 0$ for the downward flow, and counter-current flow corresponds to negative X^2 with $Y < 0$ for the upward flow and $Y > 0$ for the downward flow. As can be seen in Fig. 9, the triple solutions for the upward flow ($Y < 0$) was obtained for negative values of X^2 corresponding to the counter-current flow in an inclined pipe. However, for a downward flow ($Y > 0$) a single solution can be obtained by solving Eq. (9). This result is different from gas/Newtonian liquid flows. Previous work by Ullmann et al. (2003b) shows that triple solutions for the in situ volume fraction are obtained in a downward flow in the range of high value X^2 for gas/Newtonian liquid stratified flow, although the single solution can also be obtained in the case of a low value X^2.

Fig. 10 shows a comparison of the theoretical predictions obtained for the average void fraction with experimental data in co-current downward inclined flows in a stratified flow regime. The number of experimental points used in the correlation is about 110 and the theoretical model can describe the majority of the experimental data within ±20%. However the model fails to predict the lower end values of ε. The error may be caused by two reasons: (a) the model was simplified with a constant liquid height; and (b) a one-dimensional method cannot correctly simulate the complex nature of this flow regime because there are secondary flows and the waves observed are complex in nature (Andritsos and Hanratty, 1987).

5.2.2. Intermittent flow

Fig. 11 illustrates the effect of liquid properties on the average void fraction in a horizontal intermittent flow at constant superficial liquid velocity. It can be concluded from the experiments, as shown in Fig. 11 that for

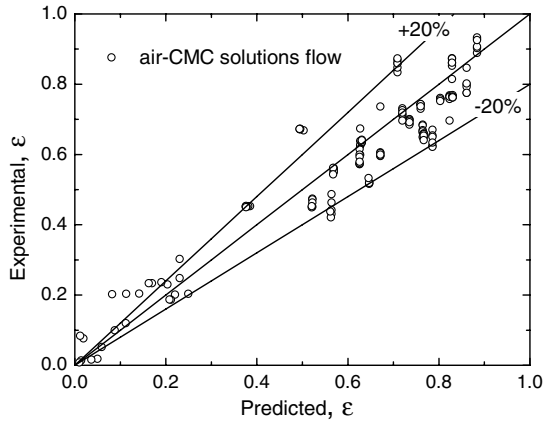

Fig. 10. Comparison of the theoretical predictions for the average void fraction with experimental data in co-current downward inclined flows in stratified flow regime.

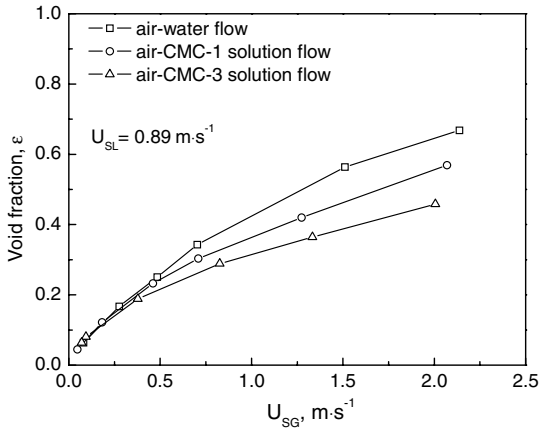

Fig. 11. The effects of liquid properties on void fraction in a horizontal intermittent flow.

air-CMC solutions flows, the average void fraction increases with an increase in the superficial air velocity, and this characteristic is similar to the one of air-water flow. However, Fig. 11 also reveals the interesting result that the average void fraction decreases for a given U_{SG} as the liquid becomes more shear-thinning (i.e. lower value of n_0) and that the deviation from the curve of gas/Newtonian liquid flow becomes gradually greater with increased U_{SG}. The reasons for the discrepancies between the gas/non-Newtonian liquid and gas/Newtonian liquid flows may be as follows:

(a) Due to the considerable differences in physical properties (particularly viscosity) of non-Newtonian and Newtonian liquids, the relative velocity ($|U_G - U_L|$) within gas/non-Newtonian liquid is higher than that within gas/Newtonian liquid flows in horizontal and upward inclined flows.
(b) Based on experimental observations, the amount of bubbles dispersed within the non-Newtonian liquid is distinctly lower than that within a Newtonian liquid in an intermittent flow when having the same superficial velocities.

A comparison of the theoretical predictions obtained from the Eq. (24) for the average void fraction with experimental data in horizontal and upward inclined flows in an intermittent flow regime is shown in Fig. 12. The number of experimental points used in the correlation is about 350, and Eq. (24) can describe the majority

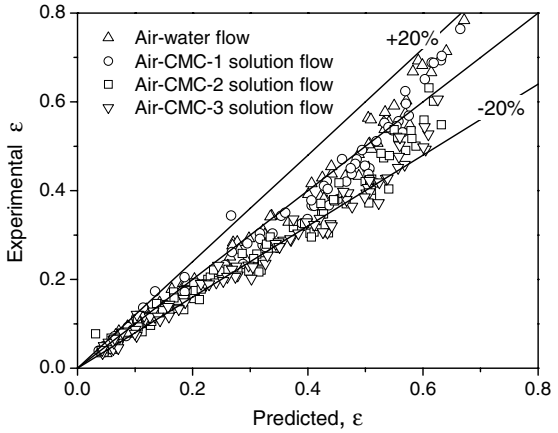

Fig. 12. Comparison of the theoretical predictions obtained from Eq. (24) for the average void fraction with experimental data in horizontal and upward inclined flows in an intermittent flow regime.

Table 3
Statistical parameters for experimental and predicted average void fraction with the Farooqi and Richardoson model (1982) for horizontal and upward intermittent flows

Inclination angle, α	0°	5°	15°	30°	75°
Average error, $E1$, (%)	0.15	4.9	4.86	18.92	10.61
Average absolution error, E2, (%)	12.3	17.91	19.26	25.86	20.67

of the experimental data within ±20%. However, it can be seen that this equation over-estimates the value of the average void fraction of gas/non-Newtonian liquid flow, especially for the liquid phase with the lower flow behaviour index, n_0. The main reason for this larger discrepancy is that Eq. (24) was solved assuming the conditions of a Newtonian liquid, not those of a non-Newtonian liquid, because for gas/non-Newtonian liquid flow, no reliable methods exist for the calculation of the translation velocity, U_T, nor for the void fraction within the liquid slug, ε_S.

Furthermore, in the present work the experimental data is also analyzed with the Farooqi and Richardson method. Farooqi and Richardson (1982) modified the Lockhart and Martinelli (1949) parameter, X, in order to analyze their holdup data for gas/non-Newtonian liquid flow. They proposed a correction factor, J, to be applied to the parameter, X, so that a modified parameter X_{MOD} is defined as

$$X_{MOD} = J \cdot X, \quad J = (U_L/U_{LC})^{1-n_0} \tag{32}$$

where U_{LC} is the critical value of superficial liquid velocity when laminar flow ceases to exist (this value can be estimated by setting the Reynolds number equal to 2000). The results are presented in Table 3. Better fitting results are obtained for a horizontal flow with an average absolute error of 12.3%. For inclined flows the agreement was worse. The failure to predict the results in inclined flows may be due to the fact that flow regimes and pipe inclination are not considered by this model.

5.3. Two-phase pressure drop

5.3.1. Stratified flow

Fig. 13 shows the effects of the flow behaviour index, n_0 and inclination angle, Y on the dimensionless pressure gradient in a stratified flow as predicted from Eq. (15). A turbulent gas flow ($m_0 = 0.2$) is assumed. It can be seen in Fig. 13a that the dimensionless pressure gradient decreases when n_0 is reduced at high ε values, but for a low value of ε the effects of liquid phase properties on Φ_L^2 may be negligible. Because the gravitational and frictional terms in the total pressure gradient equation have opposite signs for downward inclined flows, two-phase flows may experience either pressure-gain or pressure-loss, depending upon the physical properties

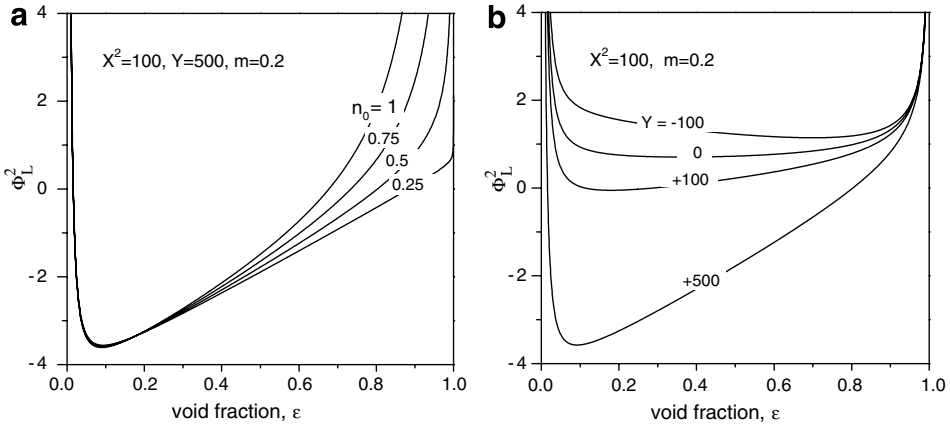

Fig. 13. The dimensionless pressure gradient, Φ_L^2 as a function of the fraction ε for stratified flow of power-law liquids in an inclined pipe.

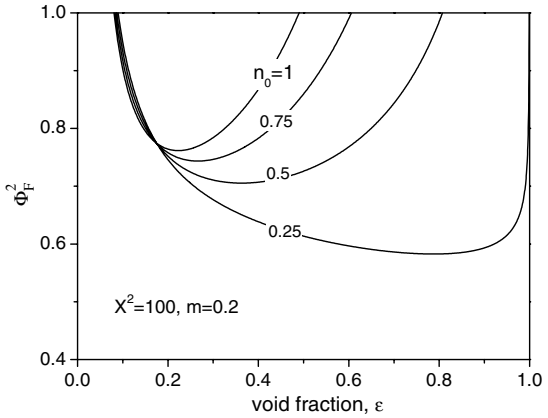

Fig. 14. The dimensionless frictional pressure gradient, Φ_F^2 as a function of the fraction ε for stratified flow of power-law liquids in a horizontal pipe.

and input fluxes of the two phases and the size and orientation of the pipe. Such behaviour is observed in Fig. 13b where for an upward inclined flow $(Y < 0)\Phi_L^2$ is generally much higher due to the hydrostatic term being positive, but the downward flow is associated with a pressure reversal phenomena since the hydrostatic pressure gradient is negative. Fig. 14 illustrates the effects of the flow behaviour index, n_0 on drag reduction in a stratified horizontal flow as predicted from Eq. (16). The dimensionless frictional pressure gradient, Φ_F^2, as a function of the void fraction ε for stratified flow of power law liquids, increases for a given ε as n_0 is increased from 0.25 to 1 over the range $0.2 < \varepsilon < 1$. The maximum drag reduction occurs at the lowest n_0 values when different liquid phases have the same superficial velocities.

The effect of channel inclination angles, α on the dimensionless frictional pressure gradient in a downward inclined stratified flow for an air-CMC-3 solution flow is shown in Fig. 15. It can be seen that the dimensionless friction pressure drop tends to reach constant values after further increases in air superficial velocity. Eq. (9) predicts, with good agreement, results for high gas superficial velocities, but fails at low gas superficial velocities and highly inclined angle. As has been previously pointed out, in those cases, ε cannot be correctly predicted and Φ_L^2 is sensitive to the predicted void fraction.

Comparison of the theoretical predictions obtained from Eq. (15) for the dimensionless frictional pressure gradient with experimental data in a downward stratified flow regime with three different pipe diameters is shown in Fig. 16. As can be observed, Φ_L^2 is generally much higher with a small diameter than with a large diameter. Considering the complex flow regime of stratified downward flow which is studied here, the

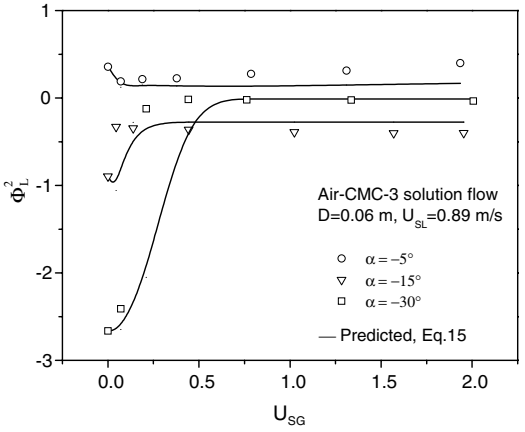

Fig. 15. The effect of channel inclination angles, α on the dimensionless frictional pressure gradient in downward inclined stratified flow for a non-Newtonian liquid/gas flow.

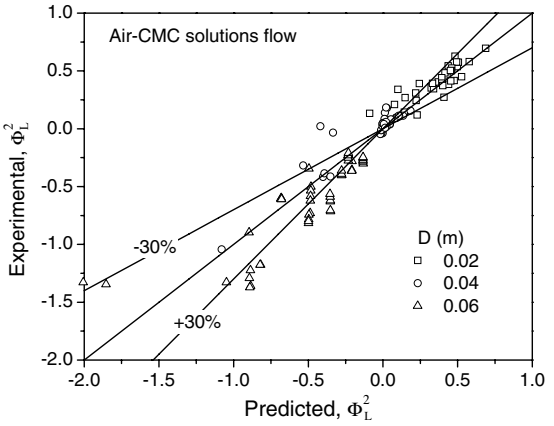

Fig. 16. Comparison of the theoretical predictions obtained from Eq. (15) for the dimensionless frictional pressure gradient with experimental data in a downward stratified flow regime.

predictions are satisfactory. The deviations in most cases are less than 30% for the dimensionless frictional pressure drop.

5.3.2. Intermittent flow

The effect of pipe inclination in upward inclined intermittent flow for an air-CMC-3 solution flow is shown in Fig. 17. The solid curves represent theoretical results and the points indicate measured values. The theoretical curve deviation from the experimental data becomes gradually greater with increased inclination angles. It should be noted that the use of a slug model for all intermittent flow regimes is questionable. Nevertheless, the overall agreement of predicted values with experimental data is very good.

The effects of pipe diameter, liquid phase properties and superficial velocity on the dimensionless frictional pressure gradient in horizontal intermittent flows are shown in Fig. 18 for air-CMC solution systems. It is well-known that for a gas/Newtonian system, Φ_F^2 increases as superficial air velocities are increased, especially at high superficial air velocities. On the contrary, Φ_F^2 decreases with increasing superficial water velocities at a given superficial gas velocity. The main reason is that the gas phase will always disturb the flow, and there will be additional pressure losses in the mixture of gas-Newtonian liquid flow. In all cases, Φ_F^2 is larger than unity in intermittent flow. However, for the gas/non-Newtonian fluid system, it can be seen in Fig. 18 that the injection of air reduces the dimensionless frictional pressure gradient for air-CMC solutions flows. The pressure drop might, in some circumstance, actually be reduced below the value for which the liquid flows alone at

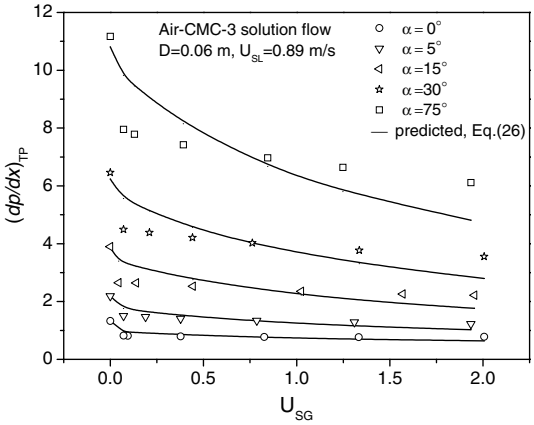

Fig. 17. The effect of channel inclination angles, α on the pressure drop in upward inclined intermittent flows for a non-Newtonian liquid/gas flow.

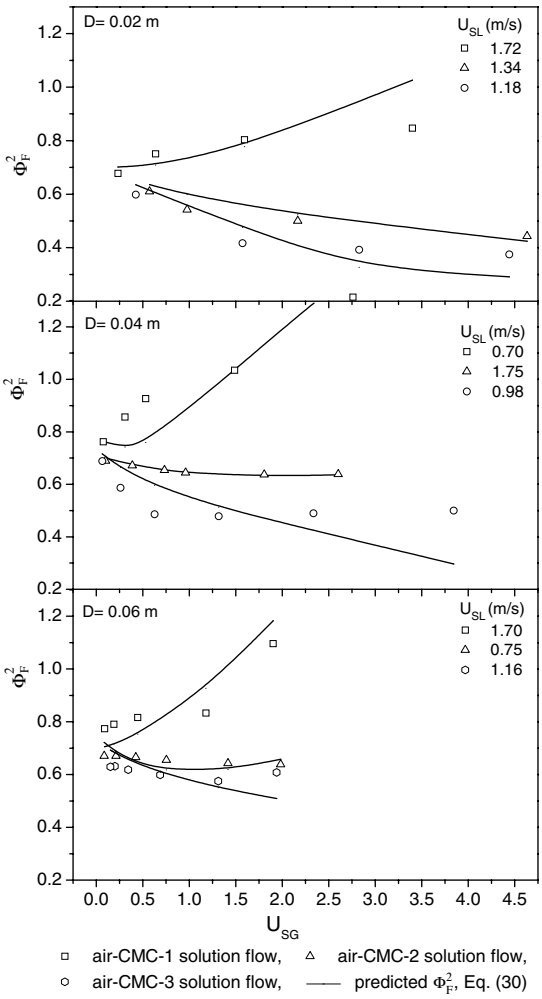

Fig. 18. The effects of liquid phase properties and superficial velocities on the dimensionless frictional pressure gradient for air/non-Newtonian liquid horizontal intermittent flows in different pipe diameters and various liquid phase solutions.

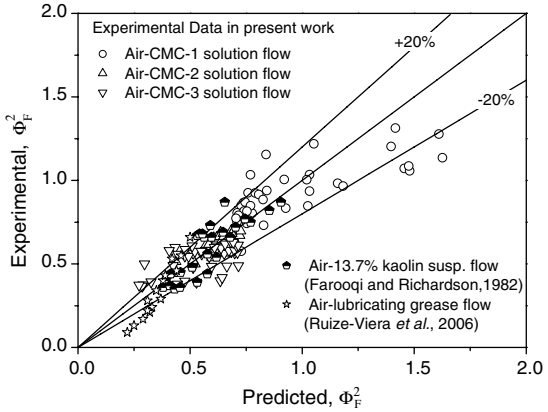

Fig. 19. Comparison of the theoretical predictions obtained from the theoretical models for the dimensionless frictional pressure gradient with experimental data in this work and for other systems reported in the literature for horizontal intermittent flow regimes.

the same superficial liquid velocity. When superficial air velocity is increased further, Φ_F^2 passes through a minimum and finally increases again until eventually exceeding unity. Furthermore, the higher fluids with shear-thinning behaviour (i.e. smaller value of flow behaviour index, n_0), the greater is the decreasing extent of Φ_F^2. As can also be observed in Fig. 18, the theoretical models allow a good prediction of the dimensionless frictional pressure gradient for air-CMC solution systems.

Fig. 19 shows a comparison of the theoretical predictions obtained from Eq. (30) for the dimensionless frictional pressure gradient with experimental data in this work and for other systems reported in the literature using a horizontal intermittent flow regime. As shown in Fig. 19, most of the experimental values are well inside the 20% deviation region, which means a reasonably good agreement between theoretical and experimental data. The proposed methods have also been verified with data collected from different references (Farooqi and Richardson, 1982 and Ruiz-Viera et al., 2006).

6. Conclusions

An experimental and theoretical study of gas–liquid two-phase flows through an inclined tube has been conducted. Special attention was given to the influence of liquid phase properties on flow pattern, void fraction and pressure drop. It was observed that the properties of non-Newtonian fluid had a minimal effect on the flow pattern in horizontal and near horizontal flows. Similar results were found for the flow of two-phase mixtures of air/non-Newtonian liquid in horizontal pipes (Chhabra and Richardson, 1984). From the experiments it can be concluded, that non-Newtonian features of liquids exert a significant effect on void fraction of two-phase mixture flows. The data shows that the average void fraction decreases for a pair of given U_{SG} and U_{SL} as the liquid becomes more shear-thinning. This may be due to the relative velocity ($|U_G - U_L|$) within a gas/non-Newtonian liquid being higher than that within a gas/Newtonian liquid. More detailed experimental and theoretical studies are needed to confirm this assumption.

The Heywood–Charles model (1979) for horizontal flow is modified for stratified flow in an inclined pipe for the average void fraction and pressure drop of the mixture flow of a gas/non-Newtonian liquid. Predictive models of void fraction and dimensionless pressure drop were presented for the stratified flow of gas and non-Newtonian liquid obeying the power-law model. Experimental data for stratified downward flows were used to verify the model. The comparisons with the experimental data showed that the model presented here provided a reasonable estimate of the average void fraction and corresponding pressure drop. The pressure drop gradient model of Taitel and Barnea (1990) for a gas/Newtonian liquid slug flow is extended to liquids possessing shear-thinning laminar flow behaviour in inclined pipes. The proposed models were tested extensively against air/different CMC solutions flows over wide ranges of inclination angles and pipe diameters. A very good agreement was obtained between the predicted and experimental results. The predicted dimensionless pressure drop matched the experimental data with less than a 20% average error. The average deviation of the predicted

void fraction from the experimental values did not exceed 20%. These results substantiate the general validity of the model presented for gas/non-Newtonian two-phase intermittent flows.

Acknowledgements

The authors gratefully acknowledge that the work described here was financially supported by the important S&T cooperation project sponsored by the Chinese Academy of Sciences and the China National Off-Shore Oil Corp. during the 11th "five year plan" (No. KJCX2-YW-L02).

References

Andritsos, N., Hanratty, T.J., 1987. Influence of interfacial waves in stratified gas–liquid flows. AIChE J. 33, 444–454.

Ansari, A.M., Sylvester, N.D., Shoham, O., Brill, J.P., 1994. A comprehensive mechanistic model for upward two phase flow in wellbores. SPE Prod. Facil., 143–152, May.

Barnea, D., 1987. A unified model for predicting flow-pattern transitions for the whole range of pipe inclinations. Int. J. Multiphase Flow 13, 1–12.

Bendiksen, K., 1984. An experimental investigation of the motion of long bubbles in inclined tubes. Int. J. Multiphase Flow 10, 467–483.

Chhabra, R.P., Farooqi, S.I., Richardson, J.F., 1984. Isothermal two-phase of air and aqueous polymer solutions in a smooth horizontal pipe. Chem. Eng. Res. Des. 62, 22–31.

Chhabra, R.P., Farooqi, S.I., Richardson, J.F., Wardle, A.P., 1983. Co-current flow of air and shear-thinning suspensions in pipes of large diameter. Chem. Eng. Res. Des. 61, 56–61.

Chhabra, R.P., Richardson, J.F., 1984. Prediction of flow patterns for cocurrent flow of gas and non-Newtonian liquid in horizontal pipes. Can. J. Chem. Eng. 62, 449–454.

Chhabra, R.P., Richardson, J.F., 1986. In: Cheremisinoff, N.P. (Ed.), Encyclopedia of Fluid Mechanics, vol. 3, Gulf, Houston.

Chhabra, R.P., Richardson, J.F., 1999. Non-Newtonian Flow in the Process Industries. Butterworth-Heinemann, Oxford.

Cohen, L.S., Hanratty, T.J., 1968. Effect of waves at a gas–liquid interface on a turbulent air flow. J. Fluid Mech. 31, 467–479.

Das, S.K., Biswas, M.N., Mitra, A.K., 1992. Holdup for two-phase flow of gas-non-Newtonian liquid mixtures in horizontal and vertical pipes. Can. J. Chem. Eng. 70, 431–437.

Dziubinski, M., 1995. A general correlation for the two-phase pressure drop in intermittent flow of gas and non-Newtonian liquid mixtures in a pipe. Trans. Chem. Eng. Res. Des. 73, 528–533.

Dziubinski, M., Fidos, H., Sosno, M., 2004. The flow pattern map of a two-phase non-Newtonian liquid–gas flow in the vertical pipe. Int. J. Multiphase Flow 30, 551–563.

Eisenberg, F.G., Weinberger, C.B., 1979. Annular two-phase flow of gases and non-Newtonian liquids. AICHE J. 25, 240–246.

Farooqi, S.I., Heywood, N.I., Richardson, J.F., 1980. Drag reduction by air injection for highly shear-thinning suspensions in horizontal pipeflow. Trans. IChemE 58, 16–27.

Farooqi, S.I., Richardson, J.F., 1982a. Horizontal flow of air and liquid (Newtonian and non-Newtonian) in a smooth pipe. Part I: A correlation for average liquid holdup. Trans. IChemE 60, 292–322.

Farooqi, S.I., Richardson, J.F., 1982b. Horizontal flow of air and liquid (Newtonian and non-Newtonian) in a smooth pipe. Part II: Average pressure drop. Trans. IChemE 60, 323–333.

Gregory, G.A., Nicholson, M.K., Aziz, K., 1978. Correlation of the liquid volume fraction in the slug for horizontal gas–liquid slug flow. Int. J. Multiphase Flow 4, 33–39.

Gomez, L.E., Shoham, O., Schmidt, Z., Chokshi, R.N., Northug, T., 2000. Unified mechanistic model for steady-state two-phase flow: horizontal to vertical upward flow. SPE J. 5, 339–350.

Hetsroni, G., 1982. Handbook of Multiphase Systems. Hemisphere publishing corp., USA.

Heywood, N., Charles, M.E., 1979. The stratified flow of gas and non-Newtonian liquid in horizontal pipes. Int. J. Multiphase Flow 5, 341–352.

Johnson, A.B., White, D.B., 1993. Experimental determination of gas migration velocities with non-Newtonian fluids. Int. J. Multiphase Flow 19, 921–941.

Kaminsky, R.D., 1998. Predicting single-phase and two-phase non-Newtonian flow behavior in pipes, Energy Resource Technology. AICHE J. 120, 2–7.

Kaya, A.S., Sarica, C., Brill, J.P., 1999. Comprehensive mechanistic model of two-phase flow in deviated wells. SPE Annual Technical Conference and Exhibition. SPE 56522, Oct., Houston.

Khatib, Z., Richardson, J.F., 1984. Vertical co-current flow of air and shear-thinning suspensions of kaolin. Chem. Eng. Res. Des. 62, 139–154.

Kokal, S.L., Stanislav, J.F., 1989. An experimental study of two-phase flow in slightly inclined pipes. Part II: flow pattern. Chem. Eng. Sci. 44, 665–679.

Lockhart, R.W., Martinelli, R.C., 1949. Proposed correlation of data for isothermal two-phase, two-component flow in pipes. Chem. Eng. Progress 45, 39–48.

Mahalingam, R., Valle, M.A., 1972. Momentum transfer in two-phase flow of gas-pseudo-plastic liquid mixtures. Ind. Eng. Chem. Fundam. 11, 470–477.

Mandhane, J.M., Greogy, G.A., Aziz, K., 1974. A flow pattern map for gas–liquid flow in horizontal pipes. Int. J. Multiphase Flow 1, 537–553.

Mukherjee, H., 1979. An Experimental Study of Inclined Two-Phase Flow. Ph.D. thesis, University of Tulsa, Tulsa, USA.

Oddie, G., Shi, H., Durlfosky, L.J., Aziz, K., Pfeffer, B., Holmes, J.A., 2003. Experimental study of two and three phase flows in large diameter inclined pipes. Int. J. Multiphase Flow 29, 527–558.

Oliver, D.R., Young-Hoon, A., 1968. Two-phase non-Newtonian flow. Part I: Pressure drop and holdup. Trans. IChemE 46, 106–115.

Petalas, N., Aziz, K., 2000. A mechanistic model for multiphase flow in pipe. J. Can. Pet. Tech. 39, 43–55.

Ruiz-Viera, M.J., Delgado, M.A., France, J.M., Sánchez, M.C., Gallegos, C., 2006. On the drag reduction for the two-phase horizontal pipe flow of highly viscous non-Newtonian liquid/air mixtures: case of lubricating grease. Int. J. Multiphase Flow 32, 232–247.

Shoham, O., 1982. Flow pattern transitions and characterization in gas–liquid two phase flow in inclined pipes. Ph.D. thesis, Tel-Aviv University, Ramat-Aviv, Israel.

Stahl, P., Rudolf von Rohr, P., 2004. On the accuracy of void fraction measurements by single-beam gamma-densitometry for gas–liquid two-phase flows in pipes. Exp. Thermal. Fluid Sci. 28, 533–544.

Spedding, P.L., Nguyen, V.T., 1980. Regime maps for air–water two-phase flow. Chem. Eng. Sci. 35, 779–793.

Taitel, Y., Barnea, D., 1990. A consistent approach for calculating pressure drop in inclined slug flow. Chem. Eng. Sci. 45, 1199–1206.

Taitel, Y., Dukler, A.E., 1976. A model for prediction flow regime transition in horizontal and near horizontal gas–liquid. AICHE J. 22, 47–55.

Ullmann, A., Zamir, M., Gat, S., Brauner, N., 2003b. Multi-holdups in co-current stratified flow in inclined tubes. Int. J. Multiphase Flow 29, 1565–1581.

Xiao, J., Shoham, O., Brill, J., 1990. A comprehensive model for two-phase flow in pipelines. The 65th SPE Annual Technical Conference and Exhibition, SPE 20631, Sep. New Orleans.

Zhang, H.Q., Wang, Q., Sarica, C., Brill, J.P., 2003a. Unified model for gas–liquid pipe flow via slug dynamics. Part 1: Model development. J. Energy Res. Tech. 125, 266–273.

Zhang, H.Q., Wang, Q., Sarica, C., Brill, J.P., 2003b. Unified model for gas–liquid pipe flow via slug dynamics. Part 2: Model validation. J. Energy Res. Tech. 125, 274–283.